Vol. **110** (2006) *ACTA PHYSICA POLONICA A* No. 2

Proceedings of the XXXV International School of Semiconducting Compounds, Jaszowiec 2006

Spin-Dependent Phenomena in (Ga,Mn)As Heterostructures

P. Sankowski and P. Kacman

Institute of Physics, Polish Academy of Sciences
al. Lotników 32/46, 02-668 Warszawa, Poland

A model for spin-dependent tunneling in semiconductor heterostructures, which combines a multi-orbital empirical tight-binding approach with a Landauer–Büttiker formalism, is presented. Using this approach we explain several phenomena observed in modulated structures of (Ga,Mn)As, i.e., large values of the electron current spin polarization in magnetic Esaki–Zener diode and the high tunneling magnetoresistance ratio. Next, the relevance of this theory to assess the tunneling anisotropic magnetoresistance effect is studied. The results of applying the tight-binding model to describe the recently observed interlayer exchange coupling in (Ga,Mn)As-based superlattices are also shown.

PACS numbers: 75.50.Pp, 72.25.Hg, 73.40.Gk

1. Introduction

Gallium arsenide doped with manganese is a flag member of the group of semiconductors which at low temperatures exhibit ferromagnetism. These so-called diluted ferromagnetic semiconductors are mainly III–V compounds with part of the cations substituted by magnetic ions. Since the discovery of such materials at the 90-ties of previous century, the ferromagnetic p-type (Ga,Mn)As is by far the most studied and best understood — for (Ga,Mn)As also the highest temperature of the transition to the ferromagnetic phase (173 K) has been achieved [1]. (Ga,Mn)As owes his unique position to the ability to form high quality junctions with nonmagnetic GaAs or AlAs, due to similar crystal structure of these compounds. Intensive studies of such multilayers with modulated magnetization have proven that most of the phenomena essential for realizing functional spintronic devices can be observed also in these all-semiconductor heterostructures. These include first of all an efficient electrical injection of spin-polarized carriers — spin injection from p-(Ga,Mn)As into nonmagnetic semiconductor has been achieved

first for spin-polarized holes [2], next a spin-polarized electron current was obtained via interband tunneling in a p-(Ga,Mn)As/n-GaAs Zener–Esaki light emitting diode (LED) [3]. Many other phenomena related to spin-dependent tunneling were observed in (Ga,Mn)As-based structures, e.g., the spin-dependent resonant tunneling [4] and the tunneling magnetoresistance (TMR) effect [5–8]. Recently, it was also reported that the magnetoresistance of the (Ga,Mn)As-based tunnel junctions is very sensitive to the direction of applied magnetic field. This so-called tunnel anisotropic magnetoresistance (TAMR) effect was observed when the saturation magnetization direction was changed in-plane [9–11] as well as when it was turned perpendicular to the magnetic layer [11, 12]. It was also shown that the magnetization vectors of consecutive (Ga,Mn)As ferromagnetic layers separated by nonmagnetic spacers in a multilayer structure are correlated by an interlayer coupling [13–17] and structures exhibiting giant magnetoresistance (GMR) were obtained [14].

In this paper we present a theory, which allows to describe the interlayer coupling between the (Ga,Mn)As layers as well as the spin-dependent transport in the above mentioned all-semiconductor tunnel junctions. In the diluted ferromagnetic semiconductor (Ga,Mn)As the ferromagnetism is hole-mediated and results from energy gain upon the redistribution between hole spin sub-bands [18]. Thus, the whole complexity of the (Ga,Mn)As valence bands resulting from strong spin–orbit interactions has to be taken into account in the calculations of the band spectrum of these multilayers. In our model a multi-orbital empirical tight-binding approach is used to describe correctly the band structure and energy spectrum in the studied multilayer systems. In contrast to the standard $\boldsymbol{k} \cdot \boldsymbol{p}$ method, this theory allows to describe properly the band dispersion in the entire Brillouin zone as well as the interfaces and inversion symmetry breaking. Within the tight-binding approach it is possible to take into account all the effects resulting from the electric field in the depletion zone of the junction, in particular the Rashba and Dresselhaus terms, which are very important for spin transport and spin tunneling. Due to strong spin–orbit mixing one can expect in (Ga,Mn)As-based structures the spin diffusion length to be shorter and comparable to the phase coherence length. This makes the models based on the diffusion equation, which describe well the spin tunneling phenomena in metallic junctions, non-applicable to the structures consisting of (Ga,Mn)As layers. Thus, to describe the spin-dependent tunneling in various (Ga,Mn)As-based semiconductor heterostructures with modulated magnetization we consider vertical spin coherent transport within the Landauer–Büttiker formalism.

2. Interlayer coupling and the tight-binding model

For magnetic metallic thin film structures it has been shown that the phenomenon, which leads to the giant magnetoresistance effect and many applications [19], i.e., the interlayer exchange coupling (IEC) results from the spin dependent

changes of the density of states due to the quantum interference of conduction electron waves [20]. It has been also proven that similar mechanism, however mediated by valence-band electrons, leads to long-range magnetic correlations also when there are no free carriers in the system [21]. The mediated by valence-band electrons IEC, i.e., superexchange-type interaction, has been shown to lead in all-semiconductor EuS- and EuTe-based superlattices to antiferromagnetic (AFM) correlations between successive magnetic layers [21–23], in agreement with the experimental observations. In this tight-binding approach the interlayer coupling is determined by the difference ΔE between the total energies of valence electrons calculated for two superlattice configurations: with spins in consecutive magnetic layers aligned parallel and antiparallel. The preferred spin configuration is given by the sign of ΔE — the negative value corresponds to ferromagnetic (FM) IEC whereas the positive sign indicates an AFM correlation.

In contrast, in the (Ga,Mn)As-based semiconductor ferromagnetic/nonmagnetic systems interlayer coupling of opposite FM sign was observed — by magnetic measurements [13–15], neutron diffraction [16], and polarized neutron reflectometry [17]. These structures differ from the previously considered EuS-based ferromagnetic semiconductor multilayers by many aspects, which all can affect the IEC. Most importantly, (Ga,Mn)As is not a magnetic but diluted magnetic semiconductor — in this ternary alloy the ferromagnetism is carrier-induced [18] and requires a considerable amount of free holes in the (Ga,Mn)As valence band. Taking this into account, a model for IEC in (Ga,Mn)As/(Ga,Al)As superlattices, constructed in the spirit of Ref. [21], has been proposed [24].

In order to construct the empirical tight-binding Hamiltonian matrix for the (Ga,Mn)As/(Ga,Al)As superlattices one has to start from the description of the constituent materials. For the band structure of bulk GaAs and AlAs the $sp^3d^5s^*$ parameterization (20 orbitals for each anion and cation), with the spin–orbit coupling included, as proposed by Jancu et al. [25] has been used in [24]. The parameterization includes only the nearest neighbor (NN) interactions. Still, it reproduces correctly the obtained by empirically corrected pseudopotential method effective masses and the band structure of GaAs and AlAs in the whole Brillouin zone. The presence of Mn ions in (Ga,Mn)As is taken into account only by including the $sp{-}d$ exchange interactions within the virtual crystal and mean-field approximations. The values of the exchange constants are determined by the experimentally obtained spin splittings: $N_0\alpha = 0.2$ eV of the conduction band and $N_0\beta = -1.2$ eV of the valence band [26]. As the valence-band structure of (Ga,Mn)As with small fraction of Mn has been shown to be quite similar to that of GaAs [26], the other parameters of the model for the (Ga,Mn)As material are taken to be the same as for GaAs. We construct the tight binding matrix for the superlattice taking for each two (cation + anion) monolayers of the structure the description of the corresponding bulk material. The NN interactions between GaAs or AlAs and (Ga,Mn)As are described by the same parameters as the interactions

in bulk materials. Consequently, the valence band offset between (Ga,Mn)As and GaAs originates only from the spin splitting of the bands in (Ga,Mn)As.

The Fermi energy in the constituent materials is determined by summing up the occupied states over the entire Brillouin zone. The number of occupied states is determined by the assumed carrier concentration in the material. Our calculations of the Fermi energy for various hole concentrations are consistent with the corresponding results presented in Ref. [18].

The dependence of the calculated difference in the total valence electrons energy on the position of the Fermi level, i.e., the dependence of interlayer coupling constant J on the average concentration of holes p in the superlattice valence band, is presented in Fig. 1. As shown in the figure, J has an oscillatory character, but

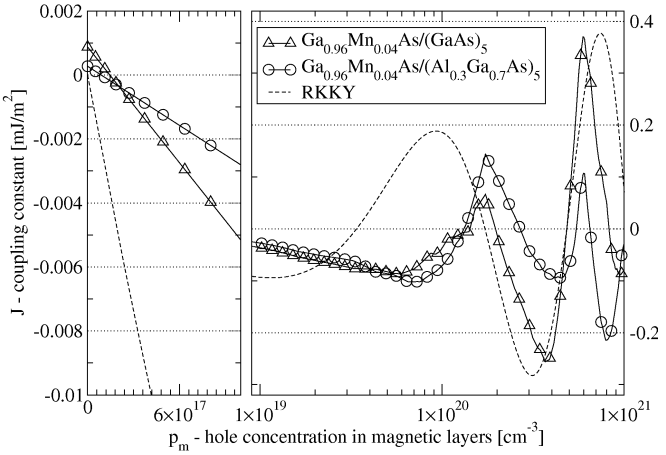

Fig. 1. The calculated dependence of interlayer coupling constant J on the hole concentration in superlattices consisting of alternating $m = 4$ $Ga_{0.96}Mn_{0.04}As$ monolayers and $n = 5$ monolayers of GaAs or $Ga_{0.7}Al_{0.3}As$. J_{RKKY} is shown for comparison. After Ref. [24].

in contrast to IEC mediated by the Ruderman–Kittel–Kasuya–Yoshida (RKKY) interaction at the limit of a hypothetical (Ga,Mn)As/GaAs superlattice with completely filled valence bands ($p = 0$) J tends not to zero, but to a finite positive value, which corresponds to AFM IEC. The careful analysis of the dependence of the calculated IEC on hole concentration and the content of Mn ions in the magnetic (Ga,Mn)As layers as well as on the nonmagnetic spacer layers material and thickness [24], shows that for the parameters of all studied experimentally structures our model leads indeed to FM IEC, as observed. Importantly, the presented in Fig. 1 results indicate also that in (Ga,Mn)As-based heterostructures the AFM coupling between FM layers could be achieved by an appropriate engineering of the multilayer structure and a proper choice of constituent materials. The model predicts that AFM IEC should be observed in superlattices in which

the hole concentration is either increased (e.g., by appropriate annealing during the MBE growth) to about 6×10^{20} cm^{-3} or kept as low as $1.5{-}2.5 \times 10^{20}$ cm^{-3}. It should be noted that in the former one can expect also high Curie temperature. The(Ga,Mn)As/(Al,Ga)As system is additionally interesting because here, due to high potential barriers in the nonmagnetic spacers, the carriers are confined in the DMS layers, which can result in strongly spin-polarized charge density.

3. Spin-dependent vertical coherent transport

To study the spin-dependent tunneling in the (Ga,Mn)As-based magnetic tunnel junctions, we consider a model heterostructure, which is uniform and infinite in the x and y directions and has modulated magnetization along the z direction. The heterostructure is connected to two semi-infinite bulk contacts denoted by L and R. The length of the simulated structure is comparable to the phase coherence length. In the presence of spin–orbit coupling the spin is not a good quantum number. The only preserved quantities in tunneling are the energy E and, due to spatial in-plane symmetry of our structures, the in-plane wave vector $k_\parallel$. Our goal is to calculate the spin-dependent current, which is determined by the transmission probability from the ingoing Bloch state at the left contact to the outgoing Bloch state at the right contact. To compute all one electron states in the device for given $k_\parallel$ and E the above described tight-binding matrix is used.

3.1. Scattering formalism and transfer coefficients

The Bloch states in the two contacts L and R are characterized by the perpendicular to the layers wave vector component $k_\perp$ and are denoted by $|L, k_{L,\perp,i}\rangle$ and $|R, k_{R,\perp,i}\rangle$, respectively. The transmission probability $T_{L,k_{L,\perp,i}\to R,k_{R,\perp,j}}$ is a function of the transmission amplitude $t_{L,k_{L,\perp,i}\to R,k_{R,\perp,j}}(E, \boldsymbol{k}_\parallel)$ and group velocities in the left and right lead, $v_{L,\perp,i}$ and $v_{R,\perp,j}$:

$$T_{L,k_{L,\perp,i}\to R,k_{R,\perp,j}}(E, \boldsymbol{k}_\parallel) = \left|t_{L,k_{L,\perp,i}\to R,k_{R,\perp,j}}(E, \boldsymbol{k}_\parallel)\right|^2 \frac{v_{R,\perp,j}}{v_{L,\perp,i}}. \tag{1}$$

The current flowing in the right direction can now be written as [27]:

$$j_{L\to R} = \frac{-e}{(2\pi)^3\hbar}\int_{\mathrm{BZ}} \mathrm{d}^2k_\parallel \mathrm{d}E f_L(E) \sum_{k_{L,\perp,i},k_{R,\perp,j},v_{L,\perp,i},v_{R,\perp,j}>0} T_{L,k_{L,\perp,i}\to R,k_{R,\perp,j}}(E, \boldsymbol{k}_\parallel), \tag{2}$$

where f_L or respectively f_R are the electron Fermi distributions in the left and right interface and i, j number the corresponding Bloch states. Plugging in the expression given in Eq. (1) and using the time reversal symmetry

$$T_{L,k_{L,\perp,i}\to R,k_{R,\perp,j}}(E, \boldsymbol{k}_\parallel) = T_{L,-k_{R,\perp,j}\to R,-k_{L,\perp,i}}(E, \boldsymbol{k}_\parallel) \tag{3}$$

we get

$$j = \frac{-e}{(2\pi)^3\hbar}\int_{\mathrm{BZ}} \mathrm{d}^2k_\parallel \mathrm{d}E \left[f_L(E) - f_R(E)\right]$$

$$\times \sum_{k_{L,\perp,i},k_{R,\perp,j},v_{L,\perp,i},v_{R,\perp,j}>0} \left|t_{L,k_{L,\perp,i}\to R,k_{R,\perp,j}}(E, \boldsymbol{k}_\parallel)\right|^2 \frac{v_{R,\perp,j}}{v_{L,\perp,i}}. \tag{4}$$

Let us define the spin polarization of the outgoing Bloch state as

$$P_{R,k_{R,\perp,i}}(E,\boldsymbol{k}_\parallel) = \langle R, k_{R,\perp,i}|\boldsymbol{\Omega}\cdot\boldsymbol{s}|R,k_{R,\perp,i}\rangle, \tag{5}$$

where $\boldsymbol{\Omega}$ is the magnetization direction vector and $\boldsymbol{s}$ is the spin operator. Then, we can define the total spin current

$$j_s = \frac{-e}{(2\pi)^3\hbar}\int_{\mathrm{BZ}} \mathrm{d}^2k_\parallel \mathrm{d}E\,[f_L(E) - f_R(E)]$$

$$\times \sum_{k_{L,\perp,i},k_{R,\perp,j},v_{L,\perp,i},v_{R,\perp,j}>0} T_{L,k_{L,\perp,i}\to R,k_{R,\perp,j}}(E,\boldsymbol{k}_\parallel)P_{R,k_{R,\perp,i}}. \tag{6}$$

The spin polarization of the coherently transmitted current is now equal to

$$P_s = \frac{j_s}{j}. \tag{7}$$

To calculate the current one has to determine the transmission probability, thus the transmission amplitude $t_{L,k_{L,\perp,i}\to R,k_{R,\perp,j}}(E,\boldsymbol{k}_\parallel)$ and the group velocities $v_{L,\perp,j}$ of the ingoing and $v_{R,\perp,j}$ of outgoing states. These can be obtained by solving the Schrödinger equation for the structure with the appropriate scattering boundary conditions, i.e., by following the method presented in Ref. [28]. We start with dividing the heterostructure into layers consisting of several atomic monolayers in such a way that the tight-binding elements are nonzero only between neighboring layers. The layers in the left lead are numbered $s \leq 0$, the internal layers are numbered $s = 1,\ldots,N$ and the layers in the right lead are numbered $s > N$. As mentioned above, the tight-binding matrix is used to compute all one electron states in the device for given $\boldsymbol{k}_\parallel$ and E. Let $\boldsymbol{C}_s$ denote the coefficients of a given state expanded into the basis orbitals in the layer s. Thus, the Schrödinger equation implies the following conditions for the states in the s-th layer:

$$(H_{s,s} - E)\,\boldsymbol{C}_s + H_{s-1,s}\boldsymbol{C}_{s-1} + H^\dagger_{s,s+1}\boldsymbol{C}_{s+1} = 0, \tag{8}$$

where $H_{s,s}$ and $H_{s,s+1}$ are the intra- and interlayer tight-binding matrices. Moreover, for the leads we need to impose the Bloch condition on the incoming wave

$$\boldsymbol{C}_s = \mathrm{e}^{\mathrm{i}k_\perp d_\perp}\boldsymbol{C}_{s-1}, \tag{9}$$

where $d_\perp$ is the width of the layer along the z direction. Similar equation can be constructed for the right lead. From these two boundary conditions we get a general eigenvalue equation for $k_\perp$ and the corresponding eigenvectors. Let us denote by $D_{L,l}$ the eigenvectors in left lead that propagate to the left, and by $D_{L,r}$ the eigenvectors propagating to the right. Similarly, we define $D_{R,l}$ and $D_{R,r}$. Now the boundary conditions are given by

$$\begin{pmatrix}\boldsymbol{C}_{-1}\\ \boldsymbol{C}_0\end{pmatrix} = \begin{pmatrix}D_{L,r} & D_{L,l}\end{pmatrix}\begin{pmatrix}\boldsymbol{I}\\ \boldsymbol{r}\end{pmatrix}, \tag{10}$$

$$\begin{pmatrix}\boldsymbol{C}_{N+1}\\ \boldsymbol{C}_{N+2}\end{pmatrix} = \begin{pmatrix}D_{R,r} & D_{R,l}\end{pmatrix}\begin{pmatrix}\boldsymbol{t}\\ \boldsymbol{0}\end{pmatrix}, \tag{11}$$

where r and t are the unknown coefficient of the scattered to the left and to the

right wave. We compute the inverses D_R^{-1} and D_L^{-1} and divide them into blocks

$$D^{-1} = \begin{bmatrix} (D^{-1})_{1,1} & (D^{-1})_{1,2} \\ (D^{-1})_{2,1} & (D^{-1})_{2,2} \end{bmatrix}. \tag{12}$$

The width and the height of the block $(D^{-1})_{1,1}$ is given by the number of states propagating to right. One can now rewrite the parts of (10) and (11) as

$$\begin{bmatrix} (D_L^{-1})_{1,1} & (D_L^{-1})_{1,2} \end{bmatrix} \begin{pmatrix} \boldsymbol{C}_{-1} \\ \boldsymbol{C}_0 \end{pmatrix} = \boldsymbol{I}, \tag{13}$$

$$\begin{bmatrix} (D_R^{-1})_{2,1} & (D_R^{-1})_{2,2} \end{bmatrix} \begin{pmatrix} \boldsymbol{C}_{N+1} \\ \boldsymbol{C}_{N+2} \end{pmatrix} = \boldsymbol{0}. \tag{14}$$

Equations (8), (13), and (14) build a full system of linear equation for $\boldsymbol{C}_\sigma$. After solving it we determine the coefficients t and r with

$$\boldsymbol{t} = \begin{bmatrix} (D_R^{-1})_{1,1} & (D_R^{-1})_{1,2} \end{bmatrix} \begin{pmatrix} \boldsymbol{C}_{N+1} \\ \boldsymbol{C}_{N+2} \end{pmatrix}, \tag{15}$$

$$\boldsymbol{r} = \begin{bmatrix} (D_L^{-1})_{2,1} & (D_L^{-1})_{2,2} \end{bmatrix} \begin{pmatrix} \boldsymbol{C}_{-1} \\ \boldsymbol{C}_0 \end{pmatrix}. \tag{16}$$

The procedure allows also to determine the needed group velocity, which is given by

$$v_\perp = \frac{1}{\hbar}\langle \Psi|[H,z]|\Psi\rangle = -\frac{2d}{\hbar|\boldsymbol{C}_\sigma|^2}\Im\left(\boldsymbol{C}_\sigma^\dagger \mathcal{H}_{\sigma,\sigma+1}\boldsymbol{C}_\sigma \mathrm{e}^{\mathrm{i}k_\perp d}\right). \tag{17}$$

3.2. Spin-dependent Zener tunneling

The model described above has been constructed to explain the very high $\approx 80\%$ spin polarization of the injected electron current in a Zener–Esaki (LED), observed by Van Dorpe et al. [3]. By this approach the whole LED structure from Ref. [3] cannot be considered. Thus, in the calculation of the spin polarization of the interband Zener tunneling current, presented in Ref. [29], we have concentrated only on the description of the (Ga,Mn)As/GaAs interface, however, using the interface band profiles obtained by the self-consistent $\boldsymbol{k}\cdot\boldsymbol{p}$ simulations of the entire device. In particular, the self-consistently calculated electrostatic potential which describes the band bending for the voltage when the interband tunneling process starts ($V_0 = 1.81$ V), is the basis for the potential profile that is incorporated into tight-binding matrix. An additional linear potential drop ΔV across the Zener diode has been assumed, when the bias on the whole spin-LED is changed. Figure 2 shows the calculated spin polarization of the electron current P_j as a function of the bias ΔV in the Zener–Esaki tunneling diode. We see that at low bias, P_j is of the order of 0.6 and decreases rapidly with the applied bias, in good agreement with the experimental results. The direct comparison of the strong dependence of P_j on bias with the experimental results in [3] is hampered by the fact that the relation between ΔV and the total bias V applied to the device is known only from simulations. However, recent experiments of Kohda et al. [30] performed in

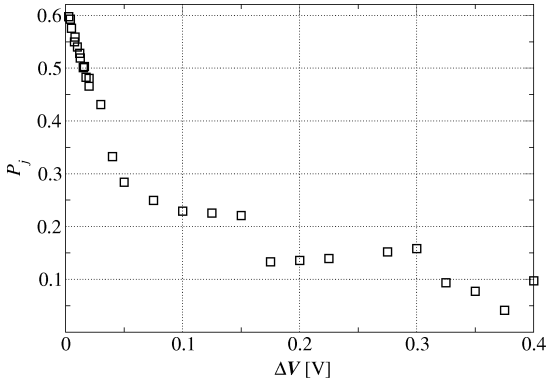

Fig. 2. The calculated bias dependence of the current polarization for the Esaki–Zener tunneling diode. After Ref. [29].

a three-contact configuration, which allows to determine the potential drop on the tunnel junction alone, fully confirm the presented in Fig. 2 results.

The magnetism in the epitaxially grown layers of (Ga,Mn)As depends strongly on both hole and manganese concentrations. It is thus obvious that also the degree of spin polarization of the tunneling current should depend crucially on these intrinsic features of (Ga,Mn)As layers. Indeed, it was shown in Ref. [31] that a higher content of magnetic ions x in $Ga_{1-x}Mn_xAs$ should increase the spin polarization of the tunneling current. In contrast, an opposite change was obtained when the hole concentration was increased. Our calculations predict also a small, about 6%, anisotropy of the spin polarization of the Zener tunneling current that reflects the symmetry of the (Ga,Mn)As/GaAs interface, in which the [110] and $[\bar{1}10]$ directions are not equivalent. A difference of this order in the spin polarization of injected current was indeed observed experimentally between the [110] and $[\bar{1}10]$ directions [29].

Finally, we have studied the anisotropy in the interband tunneling current, to assess the phenomenon discovered recently in p–n junctions with (Ga,Mn)As ferromagnetic layer and called TAMR. TAMR effect is a change in the resistance of the tunnel junction when the applied magnetic field is rotated, both in-plane [9] and out-of-plane [12]. A detailed description of our study of the in-plane and perpendicular TAMR in the p-(Ga,Mn)As/n-GaAs junction is given in Ref. [32]. Here we would like only to mention that in our model the magnitude of the Zener tunneling current, like its spin polarization described above, differs for the [110] and $[\bar{1}10]$ directions. Such in-plane TAMR, obtained even without any distortion, depends on the hole concentration in the (Ga,Mn)As layer. Although the obtained magnitude of the in-plane TAMR effect agrees with the observation in Ref. [9], it should be emphasized that in the experiment another (Ga,Mn)As/AlO_x/Au tunnel junction was measured and the change of the tunneling resistance was observed between different, [100] and [010], directions. In contrast, for the rotation of the

magnetization vector between perpendicular to the plane and in-plane directions, i.e., for the perpendicular TAMR, the calculated differences in tunneling current for both, forward as well as reverse bias, agree very well with the observed in Ref. [12].

3.3. Tunneling magnetoresistance

We have also applied our theory of spin dependent coherent tunneling to a typical TMR device, i.e., to trilayer structure with magnetic p-type $Ga_xMn_{1-x}As$ leads separated by a nonmagnetic GaAs spacer. In such structures strong TMR effect, i.e., large difference in the resistance of the device for two configurations, with parallel (FM) and the antiparallel (AFM) alignments of the magnetizations in the leads, has been observed [5, 7, 8]. The calculated within our model TMR ratio increases with the content of magnetic ions — with this dependence the TMR values observed for different samples in the above mentioned experiments can be explained [31]. Similarly to the spin polarization of the tunneling current in the Zener–Esaki diode, the observed TMR shows a rapid decay with the increase in applied bias. Our calculations reproduce such decay, as shown in Fig. 3.

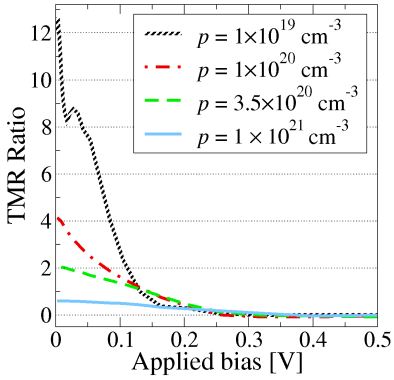

Fig. 3. The calculated bias dependence of the TMR effect in p-$Ga_{1-x}Mn_xAs$/$(GaAs)_4$/p-$Ga_{1-x}Mn_xAs$ trilayer with the spacer of $d = 4$ monolayers for different hole concentrations p and Mn ions content $x = 0.08$. After Ref. [32].

Figure 3 shows that TMR ratio and its decay with applied voltage depend strongly on the hole concentration in the magnetic layers. However, the hole concentration does not influence very much the bias where the TMR reaches zero — this voltage corresponds to the barrier height between $Ga_{0.92}Mn_{0.08}As$ and GaAs. These results suggest that the TMR and its decrease with the applied bias result predominantly from the band structure effects and can be controlled by appropriate engineering of the band offsets in the heterostructure, in particular by the content of magnetic ions in the (Ga,Mn)As layer and a proper choice of the nonmagnetic spacer. The calculated dependence of TMR on the direction of the magnetization vector is shown in Fig. 4. One can observe that for TMR only the

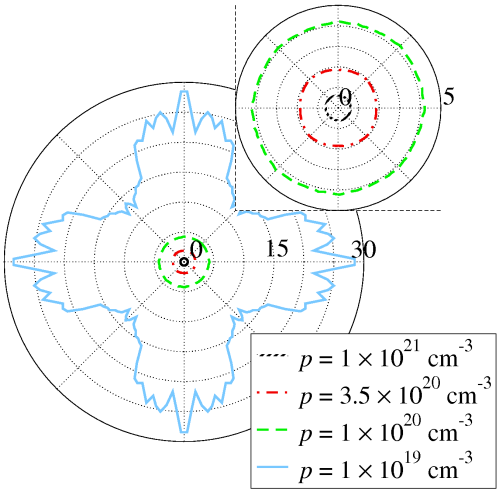

Fig. 4. Dependence of TMR ratio on the direction of in-plane magnetization for various hole concentrations in p-$Ga_{0.92}Mn_{0.08}As$/$(GaAs)_4$/p-$Ga_{0.92}Mn_{0.08}As$ trilayer structure. After Ref. [32].

[100] and [110] magnetization directions are not equivalent and the D_{2d} symmetry of the zinc-blende crystal structure is with high accuracy recovered. We recall that the calculated in the previous section anisotropy of the spin polarization of the electron tunneling current in the Esaki–Zener diode reflects the C_{2v} symmetry of a single zinc-blende interface. For the TMR ratio the symmetry is different because here two such interfaces contribute.

As shown in Fig. 4, also the in-plane anisotropy of TMR depends crucially on the concentration of holes in the magnetic layer. For hole concentrations p in the range of 10^{20} cm^{-3} the obtained anisotropy of TMR is below 10%, however, for low concentrations, $p = 10^{19}$ cm^{-3} it becomes as strong as 250%. Yet, it should be stressed that for such low concentrations hole localization effects, not taken into account in our theory, can be important. Moreover, as it has been shown in [32], the anisotropy of TMR results from the anisotropy of the current in the AFM configuration. Thus, our model does not explain the TAMR effect, which consists of a strong dependence of tunneling current on the direction magnetization in the TMR junctions in the FM configuration, as reported for some structures [10, 11].

4. Summary

A tight-binding approach is presented, which takes into account the relevant features of the band structure of the (Ga,Mn)As-based multilayers. By combining this tight-binding model with the Landauer–Bütikker formalism, we have developed a theory of spin-dependent quantum transport for spatially modulated structures of hole-controlled diluted ferromagnetic semiconductors. The model disregards disorder effects, so that it is applicable to the carrier density range and

length scales, where localization effects are unimportant. The results presented in this and our previous papers demonstrate that the observed experimentally important effects, such as interlayer coupling, large magnitudes of both spin polarization of the tunneling current in the Zener–Esaki diodes and TMR ratio in trilayer structures can be understood within the proposed model. The theory has been used not only to model the observed effects but also to predict conditions to optimize the design of (Ga,Mn)As-based devices.

Acknowledgments

The authors would like to thank T. Dietl, J. Majewski, P. Van Dorpe and W. Van Roy for fruitful collaboration in obtaining several of the reported here results. The work was partially supported by the EC project NANOSPIN (FP6-2002-IST-015728) and ERATO Semiconductor Spintronics Project of Japan Science and Technology Agency. Computations were carried out exploiting resources and software of Interdisciplinary Center of Mathematical and Computer Modelling (ICM) in Warsaw.

References

[1] K.Y. Wang, R.P. Campion, K.W. Edmonds, M. Sawicki, T. Dietl, C.T. Foxon, B.L. Gallagher, in *AIP Conf. Proc.*, Vol. 772, *Physics of Semiconductors, 27th Int. Conf. on the Physics of Semiconductors*, Eds. J. Menendez, C. Van de Walle, American Institute of Physics, New York 2005, p. 333.

[2] Y. Ohno, D.K. Young, B. Beschoten, F. Matsukura, H. Ohno, D.D. Awschalom, *Nature* **402**, 790 (1999).

[3] P. Van Dorpe, Z. Liu, W. Van Roy, V.F. Motsnyi, M. Sawicki, G. Borghs, J. De Boeck, *Appl. Phys. Lett.* **84**, 3495 (2004).

[4] H. Ohno, N. Akiba, F. Matsukura, A. Shen, K. Ohtani, Y. Ohno, *Appl. Phys. Lett.* **73**, 363 (1998).

[5] M. Tanaka, Y. Higo, *Phys. Rev. Lett.* **87**, 026602 (2001).

[6] R. Mattana, J.-M. George, H. Jaffrès, F. Nguyen Van Dau, A. Fert, B. Lépine, A. Guivarch, G. Jézéquel, *Phys. Rev. Lett.* **90**, 166601 (2003).

[7] D. Chiba, F. Matsukura, H. Ohno, *Physica E* **21**, 966 (2004).

[8] M. Elsen, O. Boulle, J.-M. George, H. Jaffres, R. Mattana, V. Cros, A. Fert, A. Lemaire, R. Giraud, G. Faini, *Phys. Rev.* **73**, 035303 (2006).

[9] C. Gould, C. Rüster, T. Jungwirth, E. Girgis, G.M. Schott, R. Giraud, K. Brunner, G. Schmidt, L.W. Molenkamp, *Phys. Rev. Lett.* **93**, 117203 (2004).

[10] C. Ruster, C. Gould, T. Jungwirth, E. Girgis, G.M. Schott, R. Giraud, K. Brunner, G. Schmidt, L.W. Molenkamp, *Phys. Rev. Lett.* **94**, 027203 (2005).

[11] A. Giddings, M. Khalid, T. Jungwirth, J. Wunderlich, S. Yasin, R. Campion, K. Edmonds, J. Sinova, K. Ito, K.Y. Wang, D. Williams, B. Gallagher, C.T. Foxon, *Phys. Rev. Lett.* **94**, 127202 (2005).

[12] R. Giraud, M. Gryglas, L. Thevenard, A. Lematre, G. Faini, *Appl. Phys. Lett.* **87**, 242505 (2005).

[13] N. Akiba, F. Matsukura, A. Shen, Y. Ohno, H. Ohno, A. Oiwa, S. Katsumoto, Y. Iye, *Appl. Phys. Lett.* **73**, 2122 (1998).

[14] D. Chiba, N. Akiba, Y. Ohno, H. Ohno, *Appl. Phys. Lett.* **77**, 1873 (2000).

[15] S.J. Chung, S. Lee, I.W. Park, X. Liu, J.K. Furdyna, *J. Appl. Phys.* **95**, 7402 (2004).

[16] W. Szuszkiewicz, E. Dynowska, B. Hennion, F. Ott, M. Jouanne, J.F. Morhange, M. Karlsteen, J. Sadowski, *Acta Phys. Pol. A* **100**, 335 (2001).

[17] H. Kępa, J. Kutner-Pielaszek, A. Twardowski, C.F. Majkrzak, J. Sadowski, T. Story, T.M. Giebultowicz, *Phys. Rev. B* **64**, 121302(R) (2001).

[18] T. Dietl, H. Ohno, F. Matsukura, *Phys. Rev. B* **63**, 195205 (2001).

[19] G.A. Prinz, *Science* **282**, 1660 (1998).

[20] P. Bruno, *Phys. Rev. B* **52**, 411 (1995).

[21] J. Blinowski, P. Kacman, *Phys. Rev. B* **64**, 045302 (2001).

[22] H. Kępa, J. Kutner-Pielaszek, J. Blinowski, A. Twardowski, C.F. Majkrzak, T. Story, P. Kacman, R.R. Galazka, K. Ha, H.J.M. Swagten, W.J.M. de Jonge, A.Yu. Sipatov, V. Volobuev, T.M. Giebultowicz, *Europhys. Lett.* **56**, 54 (2001).

[23] H. Kępa, G. Springholz, T.M. Giebultowicz, K.I. Goldman, C.F. Majkrzak, P. Kacman, J. Blinowski, S. Holl, H. Krenn, G. Bauer, *Phys. Rev. B* **68**, 024419 (2003).

[24] P. Sankowski, P. Kacman, *Phys. Rev. B* **71**, 201303(R) (2005).

[25] J.-M. Jancu, R. Scholz, F. Beltram, F. Bassani, *Phys. Rev. B* **57**, 6493 (1998).

[26] J. Okabayashi, A. Kimura, O. Rader, T. Mizokawa, A. Fujimori, T. Hayashi, M. Tanaka, *Physica E* **10**, 192 (2001).

[27] Aldo Di Carlo, P. Vogl, W. Pötz, *Phys. Rev. B* **50**, 8358 (1994).

[28] C. Strahberger, P. Vogl, *Phys. Rev. B* **62**, 7289 (2000).

[29] P. Van Dorpe, W. Van Roy, J. De Boeck, G. Borghs, P. Sankowski, P. Kacman, J.A. Majewski, T. Dietl, *Phys. Rev. B* **72**, 205322 (2005).

[30] M. Kohda, T. Kita, Y. Ohno, F. Matsukura, H. Ohno, *Appl. Phys. Lett.*, in press.

[31] P. Sankowski, P. Kacman, J. Majewski, T. Dietl, *Physica E* **32**, 375 (2006).

[32] P. Sankowski, P. Kacman, J.A. Majewski, T. Dietl, arXiv:cond-mat/0607206.